

Bulk Nanostructured Metals for Innovative Applications

RUSLAN Z. VALIEV,^{1,6} ILCHAT SABIROV,² ALEXANDER P. ZHILYAEV,^{3,4}
and TERENCE G. LANGDON^{3,5}

1.—Institute of Physics of Advanced Materials, Ufa State Aviation Technical University, Ufa 450000, Russia. 2.—IMDEA Materials Institute, Getafe 28906, Madrid, Spain. 3.—Materials Research Group, Faculty of Engineering & the Environment, University of Southampton, Southampton SO17 1BJ, UK. 4.—Institute for Metals Superplasticity Problems, Russian Academy of Science, 39 Khalturina, Ufa 450001, Russia. 5.—Departments of Aerospace & Mechanical Engineering and Materials Science, University of Southern California, Los Angeles, CA 90089-1453, USA. 6.—e-mail: rzvaliev@mail.rb.ru

Nanostructuring of various materials is a key for obtaining extraordinary properties that are very attractive for different structural and functional applications. During the last two decades, the production of bulk nanostructured materials (BNMs) by severe plastic deformation (SPD) techniques has attracted special interest since it offers new opportunities for the fabrication of commercial nanostructured metals and alloys for various specific applications. Very significant progress has been made in this area in recent years, which is evident by the first production of advanced pilot articles from nanostructured metals with new functionality. These aspects of innovations of BNMs processed by SPD are discussed in this overview.

INTRODUCTION

Nanostructuring is the new and promising method of enhancing the properties of metals and alloys for advanced structural and functional application.¹ To date, it is well established that bulk nanostructured materials (BNMs) can be produced successfully via microstructural refinement using severe plastic deformation (SPD), which is heavy straining under high imposed pressure.² SPD processing is an attractive procedure for many advanced applications as it significantly enhances the properties of a wide range of metals and alloys. Metallic materials subjected to SPD can possess not only an ultrafine-grained (UFG) structure but also specific nanostructural features, such as nonequilibrium grain boundaries (GBs), nanotwins, GB segregations, and nanoparticles. As a result, a generation of new and unusual properties has been demonstrated for a wide range of different metals and alloys, including enhanced functional (electric, magnetic, corrosion, etc.) and mechanical properties.

Since the pioneering works on producing UFG materials via SPD,³ two SPD techniques have attracted close attention and have lately experienced further development.² These techniques are high-pressure torsion (HPT) and equal-channel angular pressing (ECAP). Over the last 10–15 years, there

appeared a wide diversity of new SPD techniques: for example, accumulative roll bonding (ARB), multiaxial forging, twist extrusion, and others.^{2,4} Nevertheless, processing by HPT and ECAP has remained the most popular approach, and recently, this has acquired a new impetus through the modification of conventional die-sets and demonstrations that new opportunities are now available for using these procedures in industrial processing.⁵

A transition from laboratory-scale research to industrial applications is now starting to emerge, and many companies worldwide are involved in the research and development activities in this area. Therefore, in this article, a special emphasis is placed on the new trends in BNMs processing and forming, the principles of nanostructuring by SPD processing for superior properties, as well as the fabrication of advanced pilot articles from nanostructured metals with new functionality.

THE NEW TRENDS IN SPD PROCESSING FOR NANOSTRUCTURING OF METALS

During the last decade, SPD processing has been used successfully for a very wide range of metals and alloys^{2–7} and appropriate SPD processing routes have been developed for many commercial

alloys. The important steps required for the commercialization of SPD materials are a reduction in the processing costs and a decrease in the wastage. These two requirements have been fulfilled through the introduction of continuous processing techniques⁵ as in a combination of ECAP with the well-established conform process (ECAP-C) for the production of rods and wires. This process is illustrated in Fig. 1, and it is based on using a rotating shaft containing a groove so that the work piece is fed into the groove and is driven forward by frictional forces.⁸ This approach has a potential for processing BNMs on a commercial scale through continuous large-scale production, and this was demonstrated by establishing in Ufa a start-up company NanoMeT Ltd. (www.nano-titanium.com) for the fabrication of nanostructured Ti rods for medical use.

Recently, an alternative procedure named continuous high-pressure torsion (CHPT) was developed that may be used for the processing of strip samples as shown in Fig. 2.⁹ It was demonstrated that this as a feasible approach for extending HPT for the fabrication of larger samples. Although it is possible to achieve a nanocrystalline structure with a grain size less than 100 nm in various metals and alloys by means of HPT, for SPD processing, it is typical to form UFG structures with mean grain sizes within the submicrometer range so that, usually, the grain sizes are ~200–500 nm.^{6,7} However, other nanostructural elements are formed during SPD processing and they also affect the properties of these materials. In general, four types of nanostructured elements may be identified in SPD-processed metals and alloys using high-resolution

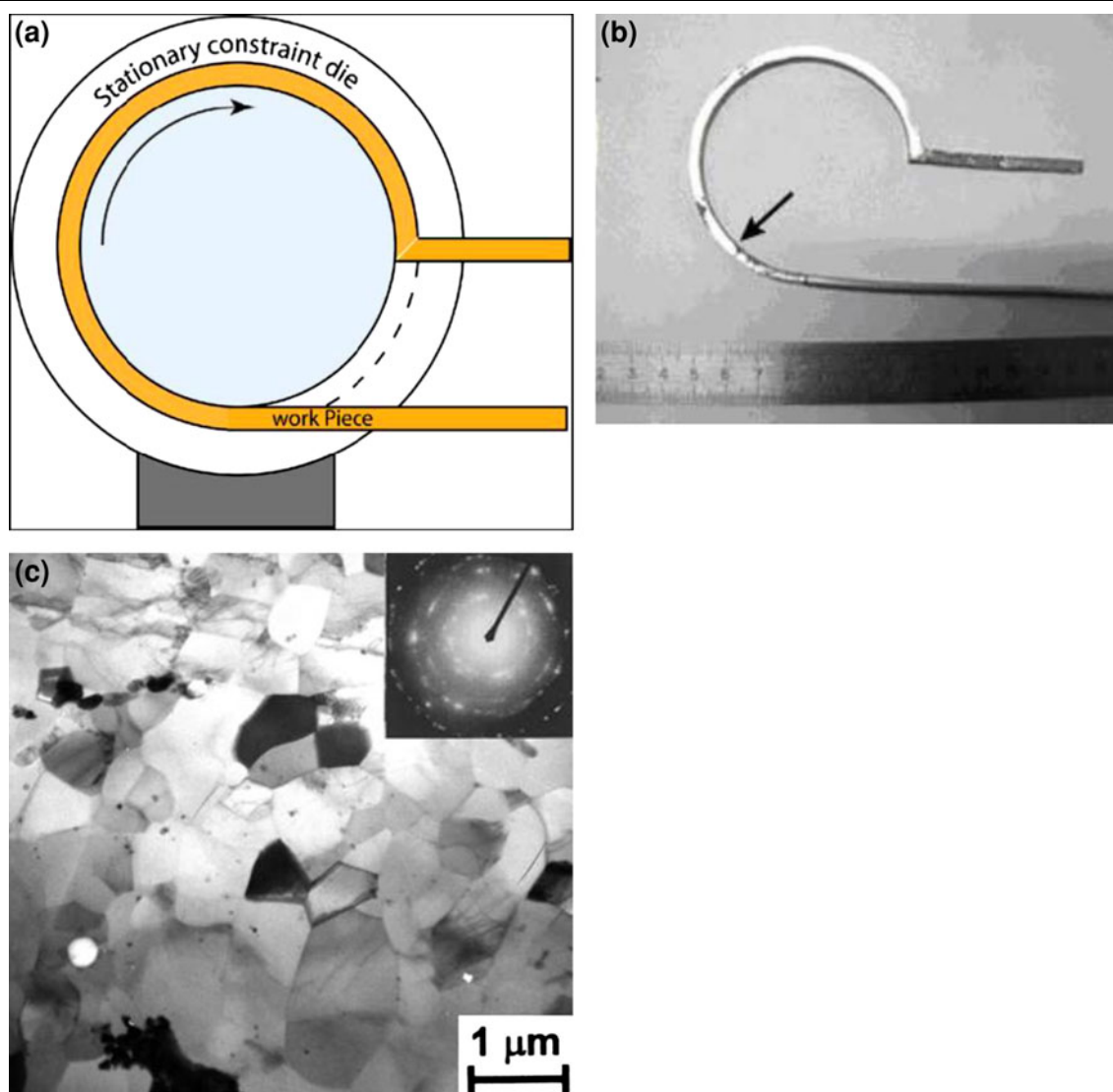


Fig. 1. (a) A schematic illustration of an ECAP-Conform setup. (b) An Al work-piece in the process of ECAP-conform where the arrow denotes the transition to a square cross-section. (c) A TEM micrograph from the longitudinal section of Al wire processed by ECAP-C through four passes.⁸

transmission electron microscopy and atom probe tomography.^{3,10} These types include the following:

- Nonequilibrium GBs that possess excess energy, long-range stresses, enhanced free volume, and with their formation associated with the interaction of lattice dislocations and GBs.^{3,11}
- Nanotwins, stacking faults, and intragranular dislocation cells that are typical of the materials after ECAP at lower temperatures and/or those subjected to additional cold rolling (CR), extrusion, or drawing.¹²
- Clusters or “clouds” of impurity segregations and alloying elements at GBs in UFG alloys processed by SPD.^{10,13} These segregations form “clouds” ~3–5 nm in size and influence the formation and motion of dislocations, which accordingly leads to additional strengthening of the alloys.
- Nanosized particles and second-phase precipitations that have been observed in many alloys subjected to SPD after solution quenching.^{6,7} The

presence of nanoparticles is related to dynamic aging and provides additional precipitation hardening of the alloys.⁷

Thus, the UFG metals and alloys processed by SPD techniques are characterized by a number of nanostructural elements that considerably influence their properties. These materials are referred to as a class of BNMs, and this definition has been accepted by the international community (www.nanospd.org).

NANOSTRUCTURED METALS AND ALLOYS WITH SUPERIOR PROPERTIES

The small grain sizes and high defect densities inherent in BNMs processed by SPD lead to much higher strengths than in their coarse-grained (CG) counterparts. During the last decade, it has been widely demonstrated that a major grain refinement, down to the nanometer range, may lead to a very high hardness and strength in various metals and alloys but nevertheless these materials invariably exhibit low ductility under tensile testing.^{4,7,14} The high strength of SPD-processed materials is usually related to the formation of the UFG structure via the well-known Hall–Petch relationship according to which the yield stress (σ_y) is calculated as

$$\sigma_y = \sigma_0 + k_y d^{-1/2} \quad (1)$$

where d is a grain size and σ_0 and k_y are constants for the material. However, it has been found in many cases that the YS value in UFG materials processed by SPD can be considerably higher than calculated according to the Hall–Petch relation.^{3,15}

Figure 3 shows the data for some Al alloys presented in the form of the Hall–Petch relation in which the YS ($\sigma_{0.2}$) is plotted against the inverse square root of the grain size ($d^{-1/2}$) for a UFG AA1100 produced by ARB-rolling as well as for an ECAP-processed Al-3% Mg alloy.^{16,17} Data obtained for the CG and UFG AA1570 and AA7475^{18,19} are also given in Fig. 3. It is seen that the YS values for the CG-quenched alloys are close to the results for the Al-3% Mg alloy. However, for the UFG materials with a grain size of 100 nm to 130 nm the value of σ_y is considerably higher than calculated from the Hall–Petch relation.

The physical nature of super strength refers to the features of the GBs formed during SPD and, in particular, to the formation of a GB segregation of alloying elements.^{13,19} In UFG materials with grain sizes of about 100 nm, the deformation mechanisms controlling the flow stress change and the process of dislocation generation occurs at the GBs and is the most difficult.¹⁹ Thus, the formation of GB segregants of alloying elements may considerably harden the dislocation emission and lead to a high-strength state.

Using the principles of GB engineering, it is possible to control the ductility of BNMs. In the UFG materials produced via SPD, GBs may vary

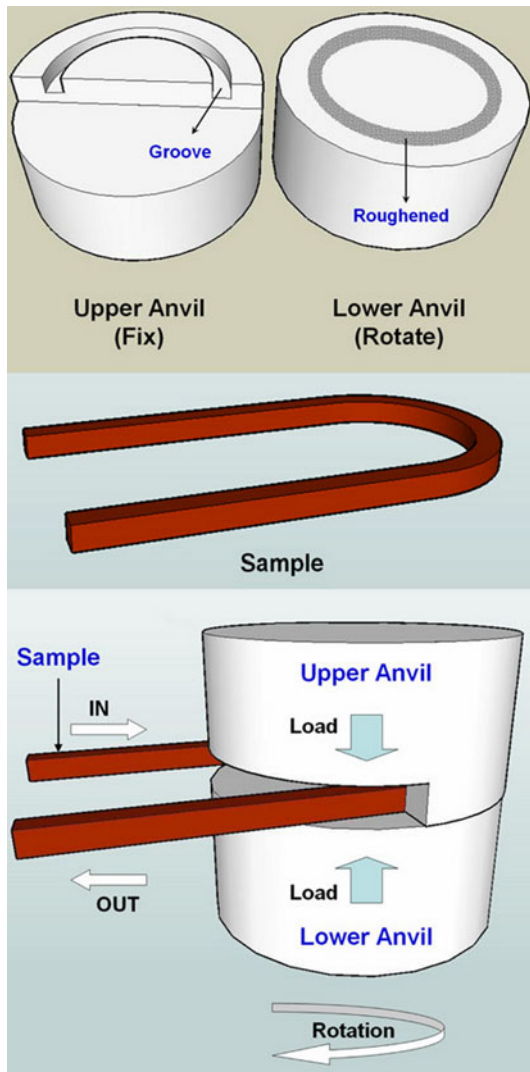


Fig. 2. Schematic illustration of the CHPT facility.⁹

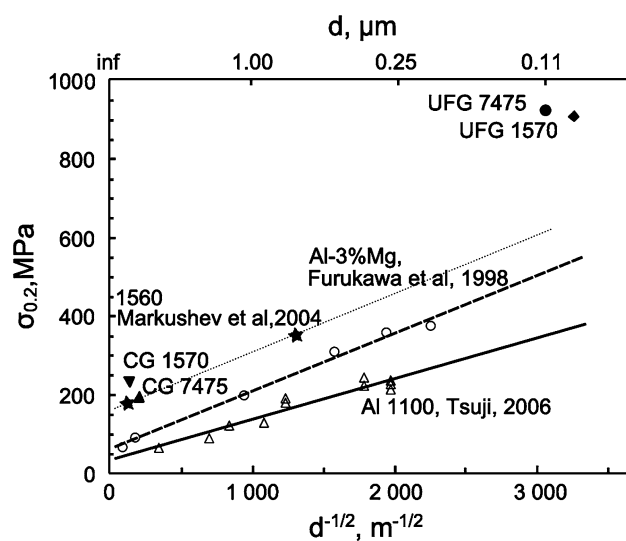


Fig. 3. The Hall-Petch relation for the AA1100,¹⁶ Al-3%Mg alloy,¹⁷ and data on the YS of the UFG AA1570¹⁸ and AA7475.¹⁹

significantly depending on the processing route, and they can belong to high- and low-angle GBs, special and random boundaries, equilibrium and nonequilibrium boundaries, as well as containing GB segregations or precipitations.^{3,10,11} In this context, there is a possibility to control and enhance the properties of UFG materials by using the principles of GB engineering.^{11,20}

The concept of GB engineering is of special interest for observations of extraordinary high strength and good ductility in bulk UFG metals produced by SPD.^{21,22} The advanced combination of high strength and high ductility, which was first revealed for nanostructured Cu and Ti²¹ and then in other metals and alloys after processing by SPD, clearly sets them apart from other CG metals. Concerning the origin of this phenomenon, it has been suggested that it is associated with an increase in the fraction of high-angle GBs with increasing straining and with a consequent change in the dominant deformation mechanisms due to the increasing tendency for the occurrence of GB sliding and grain rotation.^{11,21}

In addition, the strength and ductility are fundamental properties that are closely connected with many engineering properties of the materials, in particular fatigue, fracture toughness, durability, wear resistance, creep, and superplasticity. Such superior mechanical properties are highly desirable in the development of the next generation of advanced structural materials and during the last several years, they have been the object of innumerable investigations in the sphere of nanoSPD materials.^{2,23} The overall success of this approach means that closer attention is now directed to research into the enhancement of physical and chemical properties, such as the magnetic, electrical, and elastic properties, as well as diffusion, corrosion, and radiation resistance in UFG metals produced by

SPD.^{10,23} The origin of these properties is associated with not only the formation of UFG structure but also other microstructural elements such as nonequilibrium GBs, GB segregations, and nanophase precipitations that are characteristic of processing by SPD.

The complex structure of SPD-processed materials may result also in multifunctional properties. For example, the nanostructured TiNi alloy demonstrates an extraordinary combination of very high mechanical and functional properties including superelasticity and a shape-memory effect.²⁴ Such a combination of properties in the TiNi alloy is in contrast to its conventional CG counterpart. Another example is SPD-processed bulk magnetic materials such as Fe-Co.²⁵ Not only does the nanometer grain size of these materials induce advanced mechanical properties, but also it leads to enhanced soft magnetic properties due to the interaction of magnetic moments across the GBs.

The very high density of interfaces and short diffusion paths for point defects may result in a significantly enhanced kinetics of annealing of irradiation-induced defects in nanomaterials. In experiments with nanostructured TiNi, Ni, and Cu-0.5Al₂O₃ produced by SPD and irradiated by protons to high doses, no defects except stacking fault tetrahedra were observed, and the density of the latter was much lower than in CG polycrystals,^{10,26} illustrating clearly that nanomaterials offer an efficient resistance to radiation swelling and embrittlement. Presently, the engineering of multifunctional materials is rapidly becoming a new direction in the area of SPD nanomaterials.

RECENT DEVELOPMENTS OF BNMs FOR NEW APPLICATIONS

The application and commercialization of BNMs is associated with three potential advantages: the superior properties of BNMs, their efficient fabrication, and the possibility to produce cutting-edge products from these materials. Over the last decade, active development has been underway for fabricating pilot articles from BNMs, the shaping of which included successful realization of mechanical processing, electrochemical treatment, and superplastic forming.^{27,28} Recent reports documented more than 100 specific market areas for nanostructured metals,^{23,29} and it is evident that many of these new structural and functional applications involve extreme environments where exceptional strength and other specific properties are needed. It is interesting to consider examples of BNMs development for their innovation applications in engineering and medicine.

Nanotitanium and Ti Alloys for Biomedical Applications

Pure Ti possesses the highest biocompatibility with living organisms, but it has limited use in medicine due to its low strength. High-strength

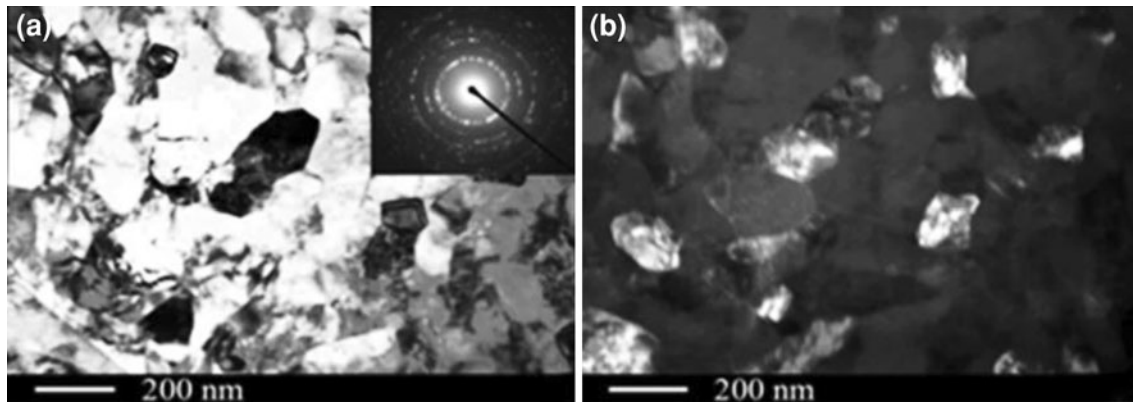


Fig. 4. TEM images of microstructure of Ti (grade 4) after ECAP-C followed by drawing (a) bright field and (b) dark field.

Table I. Mechanical properties of CP Ti (grade 4) before and after SPD processing

Condition	Yield strength (MPa)	Ultimate tensile strength (MPa)	Elongation to failure (%)
As-received condition (certificate)	589	724	27
ECAP + swaging + drawing	1150	1240	12
ECAP-C + drawing	1220	1300	11



Fig. 5. Dental implants \varnothing 3.5 mm Timplant (top) and \varnothing 2.4 mm Nanoimplant (bottom).³⁰

nanostructured pure Ti via SPD opens new avenues and concepts in medical device technology.³⁰ First, expensive and toxic alloying elements are absent in the material so that implants have better biocompatibility. Second, the implant size can be reduced to decrease the level of surgical intervention. Third, the materials exhibit improved biological reactions on their surfaces.

A new SPD-based technology has been developed recently for the fabrication of nanostructured Ti for dental implants. The processing route consists of ECAP-C, leading to grain refinement and secondary processing (swaging/drawing) providing shaping

and additional strengthening.^{30,31} Long rods with lengths up to 3 m, diameters of 4–8 mm, and accuracy grade h8 suitable for automation of implant machining can be produced using this method. These rods show a homogeneous nanostructure with a grain/subgrain size of \sim 150–200 nm (Fig. 4). The effect of this SPD processing on mechanical properties of Ti is demonstrated in Table I. It is seen that the formation of a nanostructure increases strength properties by a factor of nearly two. Fatigue studies of this material showed that fatigue strength after 10^7 fatigue cycles increases from 400 MPa in CG material up to 620 MPa in the SPD-processed material.³¹ It is noted that the mechanical properties of this nanostructured Ti are higher compared to those of conventional high-strength Ti alloys used in biomedical engineering. Nanostructuring of Ti also positively affects its biomedical properties. It accelerates colonization of the surface by fibroblast cells³⁰ and leads to increased adhesion and proliferation of bone cells due to a change of surface topography at the nanoscale.³²

The company Timplant (Ostrava, Czech Republic) used this nanostructured Ti to design and fabricate a new generation of dental implants under the trademark Nanoimplant (Timplant). These new generation implants are smaller in diameter (2.4 mm) than conventional implants (3.5 mm) (Fig. 5). Therefore, they can be successfully inserted into thin jawbones where larger implants are not feasible. Smaller dental implants also introduce less damage during the surgical intervention. To date, these implants have been certified according to the European standard EN ISO 13485:2003.

Another very promising group of materials for medical applications is nanostructured Ti-based alloys with shape memory and superelasticity effects, such as TiNi (nitinol). Nitinol is a biocompatible nickel-titanium alloy with a low elastic modulus closer to that of bone than the modulus of any other surgical metal. The low stiffness makes nitinol especially attractive as a bone replacement material since it prevents stress shielding of the ingrown and peri-implant bone. Recently, significant advances

have been made in nanostructuring TiNi alloys using HPT and ECAP techniques and in increasing the mechanical and functional properties of nanostructured TiNi alloys.^{33–35} TiNi alloys are already in use as stents, vena-cava filters, and orthodontic devices. Numerous research groups around the world have been working on the development of implantable artificial sphincters from TiNi alloys. Nanostructured, high-strength TiNi alloys are promising for further miniaturization of these medical devices.

Nanostructured Cu and Al Alloys for Prospective Electroconductors

Electrical conductivity and mechanical strength are the most important properties of conducting materials. Electrical conductivity is very sensitive to the microstructure of the material since it is determined by the scattering of electrons due to disturbances in the crystal structure including thermal vibrations, impurities, and defects. Therefore, high electrical conductivity and high strength are usually mutually exclusive in metallic materials. Pure Cu and pure Al having high electrical conductivity but very low strength serve as good examples. The alloying of these metals, strain hardening, or precipitation strengthening leads to a dramatic degradation of their electrical conductivity. For example, the electrical conductivities of some Cu alloys range from 50% to 80% of International Annealed Copper Standard (IACS) (Fig. 6). It has been demonstrated that intelligent microstructural design based on nanostructuring of Cu, Al, and their alloys via SPD processing is an attractive strategy for increasing their mechanical strength without compromising their electrical conductivity.^{36–41} Two main approaches for microstructural design have been developed.

The first approach is based on grain refinement down to an ultrafine scale and/or the introduction of nanotwins leading to increased strength. ARB was successfully utilized for grain refinement in oxygen-free copper (99.99%), in deoxidized low phosphorous Cu (Cu-0.02wt.%P-0.017wt.%Pb), and in Cu containing iron (Cu-1wt.%Fe-0.017wt.%Pb) down to 200 nm to 400 nm.³⁷ The 0.2% proof strength of these materials was increased by a factor of ~5 with just a few percent reduction in electrical conductivity, as shown on Fig. 6. Another example is bulk Cu (99.995%) having a mixed microstructure of nanograins (grain size of 66 nm) and nanoscale twins (interlamellar thickness of 44 nm) produced via dynamic plastic deformation at liquid nitrogen temperature.³⁸ Cu with this microstructure showed a yield strength an order of magnitude higher than CG materials at nearly the same electrical conductivity.

The second approach refers to minimization of the negative effect of conventional strengthening mechanisms (such as solid-solution hardening or

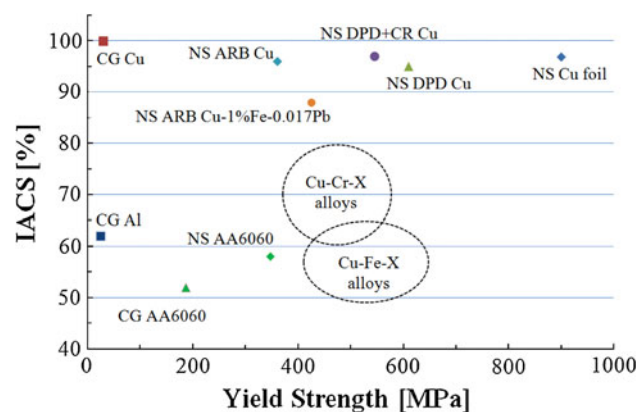


Fig. 6. Room-temperature electrical conductivity (in IACS) versus yield strength for CG Cu, CG Al, CG AA6060, some CG and Cu alloys, and their nanostructured counterparts processed via SPD. The data are taken from Refs. 37–39, and 41.

dislocation hardening) on electrical conductivity.^{39,40} It can be applied to both Cu- and Al-based alloys. A solution-treated AA6060 was subjected to HPT processing at different temperatures resulting in homogeneous nanostructures containing metastable or stable Mg_2Si particles, a varying concentration of solute atoms, and dislocation density in the microstructure.³⁹ Electrical conductivity of the processed material correlated with the concentration of solute atoms and dislocation density. The UFG material processed at 180°C showed the highest electrical conductivity very close to that of commercially pure Al that was attributed to a decreased concentration of alloying elements and the lowest dislocation density in the Al matrix, whereas its mechanical strength was significantly enhanced compared to that of the CG T6 material (Fig. 6). Similar tendencies were observed with an AA6063 alloy,³⁹ and Cu-0.7%Cr and Cu-0.7%Cr-0.9%Hf alloys.⁴⁰

Thus, nanostructuring of Cu, Al, and their alloys can significantly increase their mechanical properties with no, or very low, reduction of their electrical conductivity. HPT may be used for fabrication of small parts for electrical engineering applications whereas continuous SPD methods (such as ECAP-C) can be used for fabrication of long-length rods/wires.

Nanostructured Mg Alloys for Hydrogen Storage

The term hydrogen storage relates to methods for use H_2 as energy carrier for mobile applications. The methods cover many approaches, including high pressures, cryogenics, and chemical compounds that reversibly release hydrogen upon heating. Storing hydrogen in the solid state remains a significant technological challenge. Magnesium and magnesium alloys are considered the most attractive hydrogen storage materials because of

their high storage capacity (7.6 wt.%), light weight, and low cost. Nevertheless, high thermodynamic stability ($\Delta H = -75$ kJ/mol), high hydrogen desorption temperature ($\geq 400^\circ\text{C}$), and relatively poor hydrogen absorption–desorption kinetics at temperatures $\leq 350^\circ\text{C}$ impede the use of Mg in industrial applications.

Grain refinement can be used to improve the hydrogen storage properties of Mg. Nanosized Mg powders have been produced by mechanical alloying. Ball milling (BM) of Mg/MgH₂ gives a fine nanopowder with a grain size in the range of 10–30 nm.⁴² By reducing the grain size to nanocrystalline dimensions, the H-sorption kinetics are accelerated substantially due to the increased volume fraction of GBs, and the hydrogen desorption temperature is decreased by about 100°C.⁴³ Improved hydrogen storage capacity and kinetics are also achieved in bulk Mg-based samples via ECAP⁴⁴ and HPT.^{45,46} Figure 7 illustrates hydrating kinetic data for the nanocrystalline Mg₇₀Ni₃₀ powders milled for 1 h and 10 h, as well as for the HPT consolidated disk.⁴⁶ The as-milled powders and the HPT samples absorb hydrogen without activation, as the maximum capacity is reached after the first two absorption–desorption cycles. The maximum capacity of the powders increases with increasing milling time due to the finer microstructure and enhanced density of defects. A noticeable improvement in the H-uptake (3 wt.%) is observed in the HPT-consolidated disk. The capacity of 3 wt.% corresponds to the composition of Mg₂NiH_{3.3} and means nearly complete hydrating.

Despite major progress in using metal hybrids as hydrogen carriers, SPD may offer new technological solutions in this area. ECAP is a relatively cheap process for processing nanocrystalline elements for hydrogen batteries in the shape of cylindrical rods, and HPT may be used for processing metal hybrid tablets.

Microdevices from BNMs

In conventional CG metallic materials, the decreasing sample size may significantly affect the fundamental mechanisms of plasticity. While the plasticity of macroscopic samples appears as a smooth process, in the plastic deformation of microscopic samples, specific dislocation avalanches are formed leading to an uncontrolled deformation process including also the possibility of catastrophic failure. Therefore, fabrication of miniaturized parts or tools, particularly components for biomedical devices or microelectromechanical systems (MEMS) having geometrical features of a few micrometers, requires very careful scaling of their internal structures. The average grain size in the microparts should be smaller than the smallest dimension of the geometrical features in order to ensure their reliable property control.

Nanostructured materials lead to new directions in the fabrication of complex shape microparts for microdevices. It was recently demonstrated that hot embossing on UFG AA1050 processed via ECAP shows a good potential for the fabrication of micro-heat exchangers with geometrical features smaller than 10 μm and high thermal conductivity.⁴⁷ Hot embossing provided a very smooth embossed surface with fully transferred pattern and low failure rate of the mold, while hot embossing on CG AA1050 gave a much rougher surface with shear bands.⁴⁷ Recent experiments with micropillars of an UFG Cu-30%Zn alloy revealed a potential for avoiding intermittent flow and strain avalanches in these materials.⁴⁸

Downscaling of the SPD processing techniques together with combinations of other processing methods can dramatically ease fabrication of microparts for microdevices. An example is the use of a miniaturized ECAP die with a millimeter-scale channel to produce Al wires with grain size of 1–2 μm in a single ECAP step.⁴⁹ This ECAP

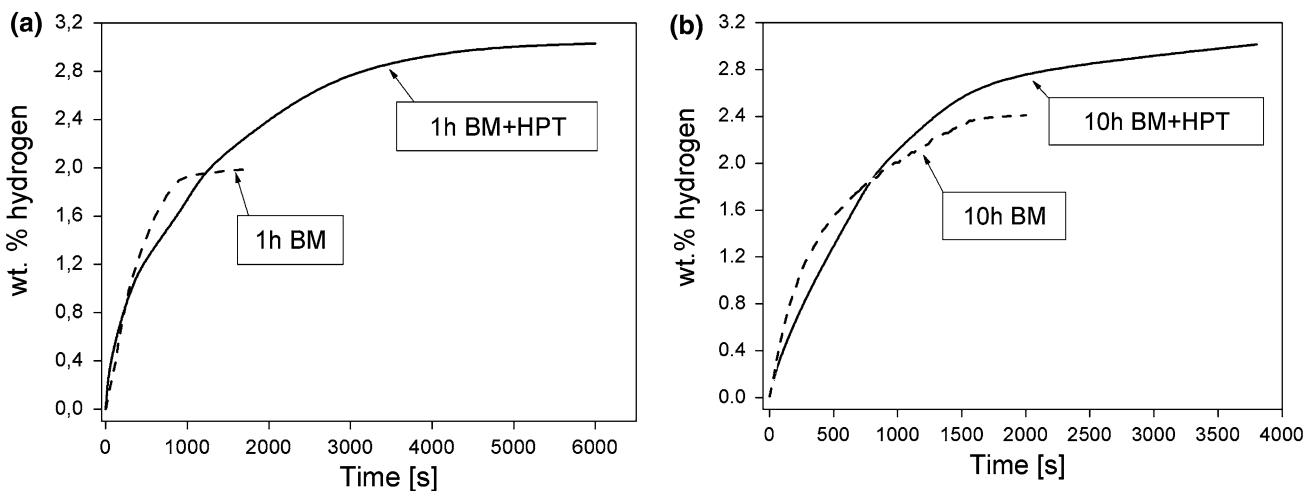


Fig. 7. Hydrogen kinetic absorption curves of Mg₇₀Ni₃₀ powder: (a) milled for 1 h and consolidated by HPT and (b) milled for 10 h and consolidated by HPT (b).⁴⁶

preprocessing can be combined with a final extrusion step where a desired axisymmetric profile can be easily imparted to the final product. An example of a possible product is a long bar with a cog-wheel profile that can be chopped into MEMS gears.²³

Nanomagnets

Advanced permanent magnets consist of hard and soft magnetic phases which are exchange-coupled at the nanoscale and, therefore, provide high storage energy. Chemical composition of phases, their size, and spatial distribution of elements in the matrix determine the magnetic properties of these materials. The SPD methods can be effectively applied for grain refinement in magnets or consolidation of magnetic nanopowders. Nanostructured RE₂Fe₁₄B (RE = Nd, Pr)-based alloys with high coercivity H_C up to 2240 kA/m were produced via HPT followed by annealing at 600°C.⁵⁰ Similar results were reported for melt-spun Nd₉Fe₈₅B₆ alloy.⁵¹ Metal-ceramic powder mixtures consisting of Co (ferromagnetic) and NiO (antiferromagnetic) phases were compacted by HPT both with and without prior BM.⁵² Enhanced coercivity of the materials was ascribed to the Co particle size refinement, the increase of stacking faults, and the magnetic coupling between Co and NiO phases.⁵²

Novel high-speed electrical machines require high-strength magnetic materials with an ultimate rupture strength ≥ 900 MPa. However, the maximum ultimate rupture strength in conventional magnets processed via rolling or high-temperature forging does not exceed 700 MPa. Recently, it was demonstrated that nanostructured Fe-25Cr-15Co and Fe-30Cr-8Co alloys with good magnetic properties and excellent mechanical properties (compression stress of 1400 MPa) may be fabricated via complex two-stage upsetting-torsion under isothermal conditions.^{53,54} These nanostructured magnetic materials could be used in developing high-speed electric machines for lower power consumption. These machines include (I) turbo generators and turbo compressors, (II) turbo molecular pumps, (III) inertial energy-storage devices, (IV) technological and medical centrifuges, and (V) electric spindles and electric drivers.

SUMMARY

Processing by SPD provides an opportunity to fabricate BNMs having attractive structural and functional applications. The latest modifications of SPD techniques can significantly increase the production rate leading to a lower price of the final (semi)products. Thus, BNMs have been already successfully used for the first application in biomedical engineering as materials for dental implants, and many new applications of BNMs in this sector are foreseen in the very near future. A very strong potential to commercialization of BNMs in electrical engineering as materials for perspective

electroconductors and in fabrication of microdevices and MEMS can be outlined. Current research activities show that SPD-processed Mg has a good potential as a material for hydrogen storage as well as nanomagnets for high-speed electric machines. It is evident that the recent considerable progress in research of BNMs provides the basis for their wide application in engineering and medicine and laboratory-scale research is now in transition towards the commercial manufacturing of nanomaterials for a range of promising products.

ACKNOWLEDGEMENTS

The work of A.P.Z. and T.G.L. was supported by the European Research Council under ERC Grant Agreement No. 267464-SPDMETALS. The work of R.Z.V. was in part supported by the Federal Special-Purpose Program under government contracts and in part by the Russian Foundation for Basic Research. I.S. acknowledges gratefully the Spanish Ministry for Science and Innovation for financial support through the Ramon y Cajal Fellowship.

REFERENCES

1. H. Gleiter, *Acta Mater.* 48, 1 (2000).
2. R.Z. Valiev, Y. Estrin, Z. Horita, T.G. Langdon, M.J. Zehetbauer, and Y.T. Zhu, *JOM* 58 (4), 33 (2006).
3. R.Z. Valiev, R.K. Islamgaliev, and I.V. Alexandrov, *Prog. Mater. Sci.* 45, 103 (2000).
4. Y. Zhu, R.Z. Valiev, T.G. Langdon, N. Tsuji, and K. Lu, *MRS Bull.* 35, 977 (2010).
5. R.Z. Valiev and T.G. Langdon, *Metall. Mater. Trans. A* 42A, 2942 (2011).
6. A.P. Zhilyaev and T.G. Langdon, *Prog. Mater. Sci.* 53, 893 (2008).
7. R.Z. Valiev and T.G. Langdon, *Prog. Mater. Sci.* 51, 881 (2006).
8. G.J. Raab, R.Z. Valiev, T.C. Lowe, and Y.T. Zhu, *Mater. Sci. Eng. A* 382A, 30 (2004).
9. K. Edalati and Z. Horita, *J. Mater. Sci.* 45, 4578 (2010).
10. X. Sauvage, G. Wilde, S.V. Divinski, Z. Horita, and R.Z. Valiev, *Mater. Sci. Eng. A* 540A, 1 (2012).
11. R. Valiev, *Nat. Mater.* 3, 511 (2004).
12. Y. Zhao, J.F. Bingert, X. Liao, B. Cui, K. Han, A.V. Sergueeva, A.K. Mukherjee, R.Z. Valiev, T.G. Langdon, and Y.T. Zhu, *Adv. Mater.* 18, 2949 (2006).
13. P.V. Liddicoat, X.Z. Liao, Y. Zhao, Y. Zhu, M.Y. Murashkin, E.J. Lavernia, R.Z. Valiev, and S.P. Ringer, *Nat. Commun.* 1, 1 (2010).
14. C.C. Koch, *Scr. Mater.* 49, 657 (2003).
15. N. Krasilnikov, Z. Pakielna, W. Lojkowski, and R. Valiev, *Solid State Phenom.* 49, 101 (2005).
16. N. Tsuji, *Nanostructured Materials by High-Pressure Severe Plastic Deformation*, ed. Y.T. Zhu and V. Varyukhin (Amsterdam: Springer, 2006), pp. 227–234.
17. M. Furukawa, Z. Horita, M. Nemoto, R.Z. Valiev, and T.G. Langdon, *Phil. Mag.* 78, 203 (1998).
18. M. Markushev and M. Murashkin, *Mater. Sci. Eng. A* 367A, 234 (2004).
19. R.Z. Valiev, N.A. Enikeev, M.Y. Murashkin, V.V. Kazhkanov, and X. Sauvage, *Scr. Mater.* 63, 949 (2010).
20. T. Fujita, Z. Horita, and T.G. Langdon, *Mater. Sci. Eng. A* 371A, 241 (2004).
21. R.Z. Valiev, I.V. Alexandrov, Y.T. Zhu, and T.C. Lowe, *J. Mater. Res.* 17, 5 (2002).
22. Z. Horita, K. Ohashi, T. Fujita, K. Kaneko, and T.G. Langdon, *Adv. Mater.* 17, 1599 (2005).

23. R.Z. Valiev, M.J. Zehetbauer, Y. Estrin, H.W. Höppel, Y. Ivanisenko, H. Hahn, G. Wilde, H.J. Roven, X. Sauvage, and T.G. Langdon, *Adv. Eng. Mater.* 9, 527 (2007).
24. V.G. Pushin, D.V. Gunderov, N.I. Kourov, L.I. Yurchenko, E.A. Prokofiev, V.V. Stolyarov, Y.T. Zhu, and R.Z. Valiev, *Ultrafine Grained Materials III* (Warrendale, PA: TMS, 2004), pp. 481–486.
25. A. Vorhauer, K. Rumpf, P. Granitzer, S. Jleber, H. Krenn, and R. Pippan, *Mater. Sci. Forum* 503–504, 299 (2006).
26. N. Nita, R. Schaeublin, M. Victoria, and R.Z. Valiev, *Phil. Mag.* 85, 723 (2005).
27. Z. Horita, M. Furukawa, M. Nemoto, A.J. Barnes, and T.G. Langdon, *Acta Mater.* 48, 3633 (2000).
28. R.Z. Valiev, R.K. Islamgaliev, I.P. Semenova, and N.F. Yunusova, *Int. J. Mater. Res.* 98, 314 (2007).
29. T.C. Lowe, *JOM* 58 (4), 28 (2006).
30. R.Z. Valiev, I.P. Semenova, V.L. Latysh, H. Rack, T.C. Lowe, J. Petruzelska, L. Dluhos, D. Hrusak, and J. Sochova, *Adv. Eng. Mater.* 10, B15 (2008).
31. R.Z. Valiev, I.P. Semenova, V.V. Latysh, A.V. Shcherbakov, and E.B. Yakushina, *Nanotechnol. Russia* 3, 593 (2008).
32. Y. Estrin, E.P. Ivanova, A. Michalska, V.K. Truong, R. Lapovok, and R. Boyd, *Acta Biomater.* 7, 900 (2011).
33. S.D. Prokoshkin, I.Y. Khmelevskaya, S.V. Dobatkin, I.B. Trubitsyna, E.V. Tatyatin, V.V. Stolyarov, and E.A. Prokofiev, *Acta Mater.* 53, 2703 (2005).
34. R.Z. Valiev, D.V. Gunderov, E.A. Prokofiev, V. Pushin, and Y.T. Zhu, *Mater. Trans.* 49, 97 (2008).
35. V.V. Stolyarov, E.A. Prokofiev, S.D. Prokoshkin, S.V. Dobatkin, I.B. Trubitsyna, I.Y. Khmelevskaya, V.G. Pushin, and R.Z. Valiev, *Phys. Met. Metallogr.* 100, 608 (2005).
36. X.H. Chen, L. Lu, and K. Lu, *J. Appl. Phys.* 102, 083708 (2007).
37. N. Takata, S.H. Lee, and N. Tsuji, *Mater. Lett.* 63, 1757 (2009).
38. Y. Zhang, Y.S. Li, N.R. Tao, and K. Lu, *Appl. Phys. Lett.* 91, 211901 (2007).
39. E.V. Bobruk, M.Y. Murashkin, V.U. Kazykhanov, and R.Z. Valiev, *Rev. Adv. Mater. Sci.* 30 (2012), in press.
40. D.V. Shangina, N.R. Bochvar, and S.V. Dobatkin, *J. Mater. Sci.*, doi:10.1007/s10853-012-6525-9.
41. L. Lu, Y. Shen, X. Chen, L. Qian, and K. Lu, *Science* 304, 422 (2004).
42. D. Fátay, Á. Révész, and T. Spassov, *J. Alloys Compd.* 399, 237 (2005).
43. G. Barkhordarian, T. Klassen, and R. Borman, *J. Alloys Compd.* 364, 242 (2004).
44. V.M. Skripnyuk, E. Rabkin, Y. Estrin, and R. Lapovok, *Int. J. Hydrogen Energ.* 34, 6320 (2009).
45. Y. Kusadome, K. Ikeda, Y. Nakamori, S. Orimo, and Z. Horita, *Scr. Mater.* 57, 751 (2007).
46. A. Revesz, Zs. Kanya, T. Verebelyi, P.J. Szabo, A.P. Zhilyaev, and T. Spassov, *J. Alloys Compd.* 504, 83 (2010).
47. X.G. Qiao, N. Gao, Z. Moktadir, M. Kraft, and M.J. Starink, *J. Micromech. Microeng.* 20, 045029 (2010).
48. N.Q. Chinh, T. Györi, R.Z. Valiev, P. Szommer, G. Varga, K. Havancsák, and T.G. Langdon, *MRS Commun.* <http://dx.doi.org/10.1557/mrc.2012.11>.
49. Y. Estrin, M. Janecek, G.I. Raab, R.Z. Valiev, and A. Zi, *Metall. Mater. Trans. A* 38A, 1906 (2007).
50. V.V. Stolyarov, D.V. Gunderov, R.Z. Valiev, A.G. Popov, V.S. Gaviko, and A.S. Ermolenko, *J. Magnet. Magnet. Mater.* 196, 166 (1999).
51. A.G. Popov, V.S. Gaviko, N.N. Shchegoleva, L.A. Shreder, D.V. Gunderov, V.V. Stolyarov, W. Li, L.L. Li, and X.Y. Zhang, *J. Iron. Steel Res. Int.* 13, 160 (2006).
52. E. Menéndez, J. Sort, V. Langlais, A. Zhilyaev, J.S. Muñoz, S. Suriñach, J. Nogués, and M.D. Baró, *J. Alloys Compd.* 434–435, 505 (2007).
53. G.F. Korznikova and A.V. Korznikov, *Mater. Sci. Eng. A* 503A, 99 (2009).
54. A. Korneva, M. Bieda, G. Korznikova, K. Sztwiertnia, and A. Korznikov, *J. Mater. Res.* 99, 991 (2008).